Volume 10, Number 3, 2017. pp. 153-164

Jordan Journal of Physics

ARTICLE

Assessment of Human Exposures to Radiation Arising from Radon in Groundwater Samples from Parts of Abeokuta, Ogun State, Nigeria

J. A. Rabiu[a], **O. A. Mustapha**[b], **V. Makinde**[b] and **A.M. Gbadebo**[c]

[a] *Department of Physics, Federal University, Kashere, P.M.B. 0182, Gombe State, Nigeria.*
[b] *Department of Physics, Federal University of Agriculture, Abeokuta, P.M.B. 2240, Abeokuta, Nigeria.*
[c] *Department of Environmental Management and Toxicology, Federal University of Agriculture, Abeokuta, P.M.B. 2240, Abeokuta, Nigeria.*

Received on: 11/3/2017; *Accepted on: 8/8/2017*

Abstract: This study aimed at assessing the level of radiation dose arising from consumption of well-water from different parts of Abeokuta metropolis by measuring the concentrations of ^{222}Rn and ^{220}Rn in well-water samples using two types of solid state nuclear track detector; namely, CR-39 and LR-115. At each well location, water sample of 3.7ml was dispensed into two specially designed plastic cups. The two detectors were exposed to alpha particles emitted by ^{222}Rn, ^{220}Rn and their decay products emanating from each water sample for forty days. The ^{222}Rn concentration obtained ranged from 3.1 to 90.8 kBq/m^3. The statistical analysis of radon concentration showed that 94% of the wells studied had radon concentration above the United States Environmental Protection Agency's maximum contaminant level of 11.1 kBq/m^3, while none of the samples had up to 1000 kBq/m^3 above which remedial action is recommended by the European Union. The calculated ranges and means of the annual effective doses from water consumption for children and adults are 44.5-1325.7, 484.7 and 22.3-66.8, 242.3μSv/y, respectively. These results showed that radon in drinking water could constitute a radiological concern for people in the areas studied.

Keywords: Radionuclides, Radon concentration, Groundwater, Effective dose, Human exposure.

Introduction

The chemical composition of groundwater does not affect the activity concentration of ^{222}Rn. The main parameters that affect the activity concentration of ^{222}Rn in groundwater are the activity concentration of ^{226}Ra in bedrock and soil, rock porosity and the ^{222}Rn emanation efficiency [1]. The mobility of ^{222}Rn is mainly influenced by diffusion or by transport processes caused by the motion of gaseous or liquid phases [2, 3]. Due to the relatively short half-life, the distance of transport of ^{222}Rn is in the range of some metres. The disequilibrium between ^{222}Rn and other uranium series radionuclides is caused by the diffusive escape of ^{222}Rn [3]. Normally, the activity concentration of ^{222}Rn in groundwater is higher than the activity concentration of other uranium series nuclides [4].

Water from wells dug in soil aquifers usually contains 5-50 Bq /I in soils with low uranium concentrations and 10-100 Bq/I in soil with normal concentrations [5]. Radon is principally a problem in wells drilled in bedrocks that contain average or high concentrations of uranium. Uranium, on the other hand, can be a significant problem in both dug and drilled wells. [6] recommends that the limit of uranium concentration in drinking water should be below 15μg/I.

Corresponding Author: J. A. Rabiu **Email**: jamoary@yahoo.com

Studies have established the level of ^{222}Rn absorption in the gastrointestinal tract and subsequent elimination via the lungs. In about an hour, 95% of the initial ^{222}Rn exits through the lungs; therefore, the main health risk from ^{222}Rn is caused directly to the stomach. The National Research Council [7] has estimated that about 30% of the activity concentration of ^{222}Rn in the stomach was integrated in the walls of the stomach. The short-lived progenies of ^{222}Rn (^{218}Po, ^{214}Pb, ^{214}Bi and ^{214}Po) together contribute 7.7% of the effective dose caused by ^{222}Rn, assuming that they are in radioactive equilibrium with ^{222}Rn in water [8, 9]. The exception is when ^{222}Rn gas is aerated from water but ^{222}Rn daughters remain in the water. However, in this case, the dose from short-lived ^{222}Rn progenies in aerated water is still less than 10% of the dose from the ^{222}Rn in the untreated water [10].

Materials and Methods

The study area is Abeokuta, which lies between latitudes 7º 5′ N and 7º 20′ N and longitudes 3º 17′ E to 3º 27′E, is a town located in the sub-humid tropical region of South-western Nigeria (Fig. 1). Abeokuta is underlain by basement complex rocks, and the populace depend largely on municipal water supplied from the River Ogun. This source of water supply is, however, not sufficient and does not meet the demand of the populace. This surface water, which is the major source of drinking water in Abeokuta, has a very low output, especially during the dry season when the evaporation rate is high (and precipitation is lower than the annual average). Most of the commercial bottle and sachet water industries also rely on water from the municipal water corporations, thus they (commercial bottle/sachet water industries) are unable to ease the prevailing water scarcity in the area.

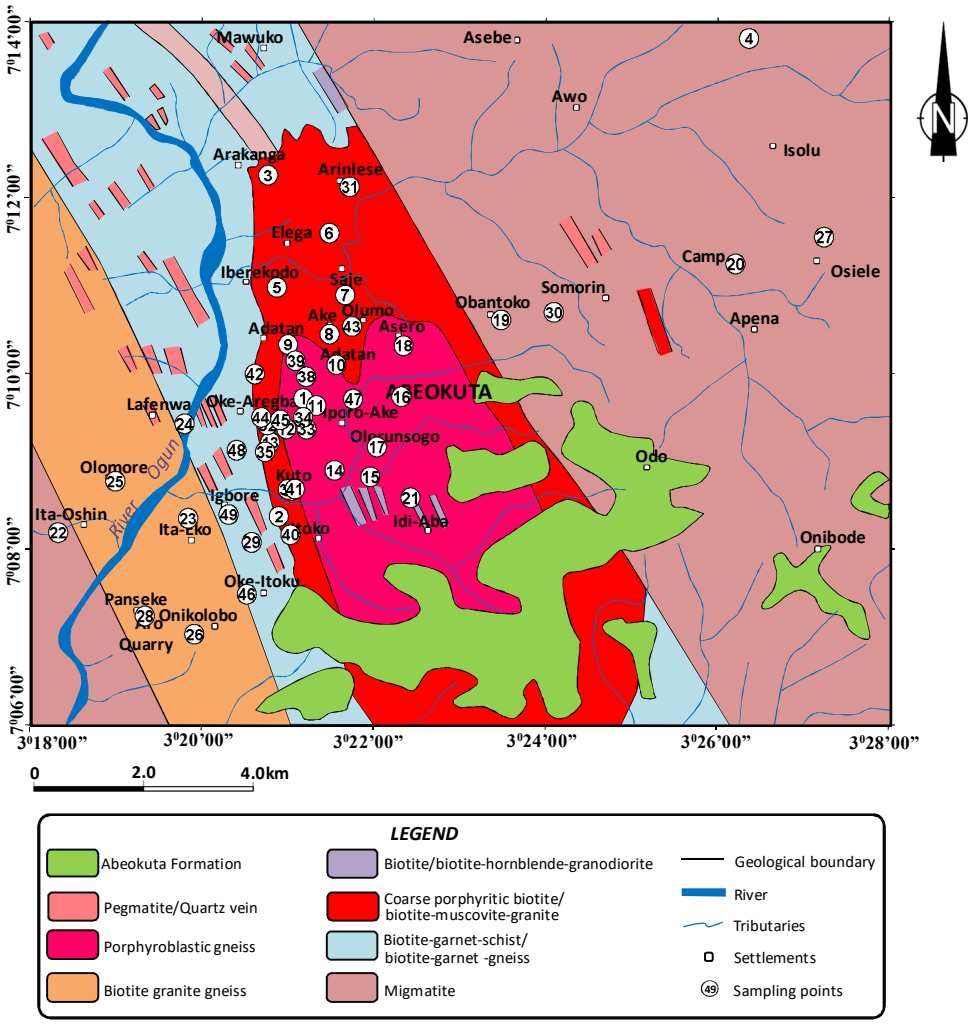

FIG. 1. Geological map of Abeokuta and its environs showing water sampling locations.

Solid State Nuclear Track Detectors (SSNTDs)

Polyallyldiglycol carbonate ($C_{12}H_{18}O_7$), known as CR-39, rigid plastic, with clear, colourless appearance and density of 1.30g.cm^{-3}, has the chemical structure shown below:

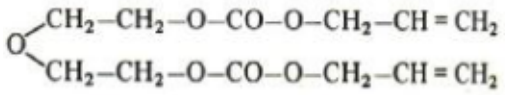

It has been used in the manufacture of eyeglass lenses since 1947. It was firstly applied during World War II to coat aircraft fuel tanks for the B-17 bomber aircraft to make them more durable. The abbreviation (CR) stands for Columbia Resin #39, because it was the 39th formula of a thermosetting plastic (Fig. 2) developed by the Columbia Resins project in 1940 [11]. The CR-39 detectors used in this study were obtained from ENEA, institute di Radio protezione, Bologna, Italy. They are rectangular with 500µm thickness.

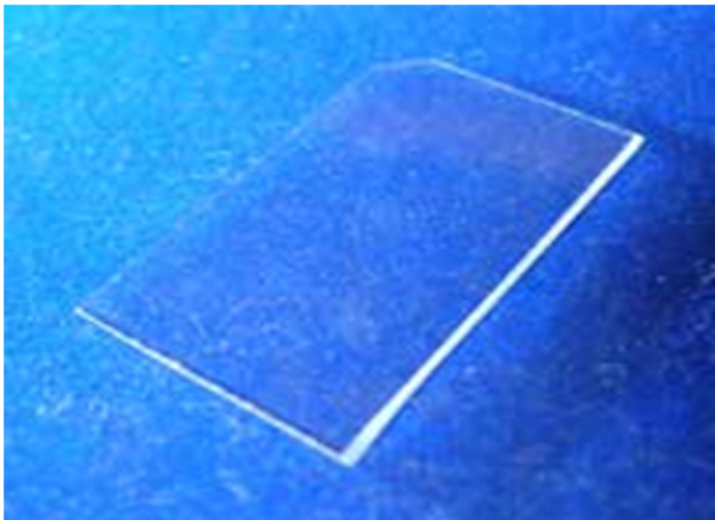

FIG. 2. Photograph of CR-39 solid state nuclear track detector (SSTND).

LR-115 Films (Type II)

LR-115 films consist of thin films of a special cellulose nitrate coloured deep red and coated on a 100µm thick polyester base. Only one side of these films is sensitive. With a needle, it gives white scratches, which must be taken into consideration when used.

LR-115 type films consist of a 100 µm thick polyester base that is coated with a 12 µm thin, α-sensitive layer of red coloured cellulose nitrate. Fig. 3 shows the red sensitive layer of the type 2 stripping film (strippable) which must be removed from the base while it is still wet at the conclusion of the washing stage. In the present study, LR-115 detectors (LR-115, Type II) were obtained from DOSIRAD, France. The detectors consist of a 12µm active layer of red cellulose nitrate on top of a 100µm clear polyester base substrate. It is a circular detector with a diameter of 2cm. It is manufactured by Kodac Pattie, France and marketed by Dosirad, France.

FIG. 3. Photograph of LR-115 film badge type II.

Experimental Method

Exposure of SSNTDs to Water Samples

Each piece of CR-39 and LR-115 detector was placed 9cm above water sample in a hermetically sealed cylindrical plastic container of radius q=2.75cm, as shown in Fig. 4. During the exposure time (40 days), α-particles emitted by radon, thoron and their corresponding daughters bombarded the SSNTD films. This setup and dimensions were based on an earlier optimization described by [12].

All the α-particles emitted by the radionuclides in the radon and thoron series, that reach the LR-115 detector under an angle lower than its critical angle of etching with a residual energy between 1.6 and 4.7 MeV, are registered as bright track-holes. The CR-39 detector is sensitive to all α particles reaching its surface under an angle smaller than its critical angle of etching (the critical angle for a detector is defined as the angle between the direction of the projectile and the normal to the detector surface, under which no track can be revealed by etching).

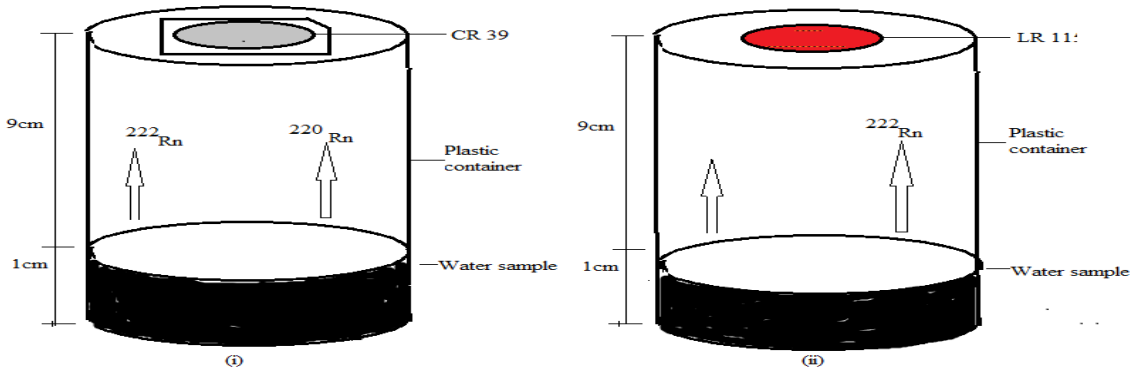

FIG. 4. Setup for measuring radon and thoron concentrations in water comprising two plastic containers (i) with CR-39 and (ii) with LR-115.

Calculation of Radon and Thoron Concentrations

Tracks of alpha-particles, emitted by the nuclei of radon and thoron series, which reached the CR-39 and LR-115 SSNTDs placed at 9cm above the water sample, were registered. The corresponding track density for each detector was calculated using the equation:

$$\text{Track Density} = \frac{\text{Average number of tracks}}{\text{area of one field of view}} . \quad (1)$$

Let *dv* represent the volume of an elementary cylinder situated between r and $r + dr$ with depth dh inside the gas volume (Fig. 5).

$$dv = 2\pi r\, dr\, dh . \quad (2)$$

Let dN_i represent the number of α-particles of index i and energy $E_{\alpha i}$ emitted from the radioactive nuclei during the exposure time t_e.

$$dN_i = \lambda_i dn_i t_e \quad (3)$$

where dn_i is the number of α-emitters of index i and radioactive decay constant λ_i in the volume dv.

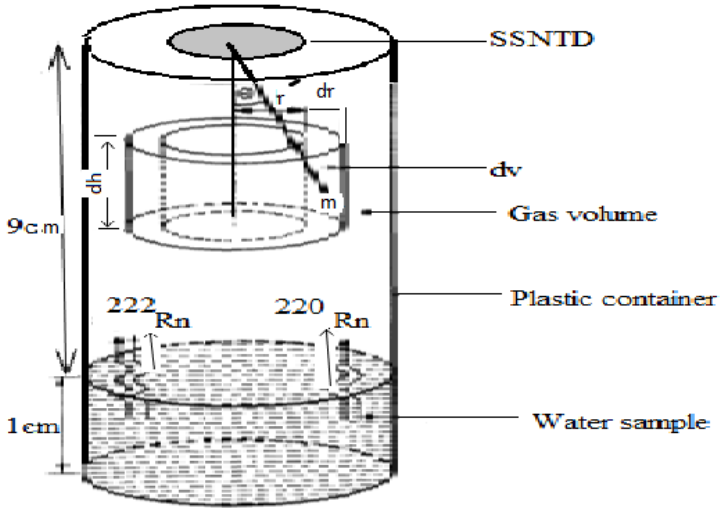

FIG. 5. Arrangement of the SSNTD films placed at a distance of 9 cm above a water sample in a cylindrical plastic container of radius q = 2 cm.

Equation (3) may be rewritten as:

$$dN_i = \lambda_i \tilde{\omega}_i dv t_e \quad (4)$$

where $\tilde{\omega}_i$ is the number of α-emitters of index i per unit volume.

Assuming a secular equilibrium between the two radionuclides (^{222}Rn, ^{220}Rn) and their corresponding daughters ($\lambda_u \tilde{\omega}_u = \cdots = \lambda_i \tilde{\omega}_i \; and \; \lambda_{Th} \tilde{\omega}_{Th} = \cdots = \lambda_i \tilde{\omega}_i$), equation (4) becomes:

$$dN_i = \lambda_{222} \tilde{\omega}_{222} 2\pi r dr dh t_e \quad (5)$$

for the ^{222}Rn family and

$$dN_i = \lambda_{220} \tilde{\omega}_{220} 2\pi dr dh t_e \quad (6)$$

for the thoron family, where λ_{222} and λ_{220} are the ^{222}Rn and ^{220}Rn decay constants, respectively.

Let P_i^{CR} represent the probability for an α-particle of energy $E_{\alpha i}$ and index i emitted at a distance x from the detector to reach and be registered on the CR-39 SSNTD [13]:

$$P_i^{CR} = \int_0^{R_i} [1 - cos\theta_c\,(x)]\, dx \quad (7)$$

where R_i is the range of the α-particle of energy $E_{\alpha i}$ and index i in gas volume and θ_c is the critical angle of etching of the CR-39 SSNTD.

The number of α-particles emitted from the radon family nuclei, in the volume dv, which reach and are registered on the CR-39 SSNTD, is given by:

$$\left.\begin{aligned} dN^{CR}(^{222}R_n) = \\ \lambda_{222} \varpi_{222} t_e 2\pi r dr \sum_{i=1}^{3} k_i P_i^{CR} dh \end{aligned}\right\} \quad (8)$$

where k_i is the branching ratio in %.

Consequently, the total number of α-particles emitted from the radon family nuclei in the whole sample which are registered on the CR-39 SSNTD is given by:

$$\left.\begin{aligned} N_T^{CR}(^{222}R_n) = \\ A_C^{222}(Bq\,cm^{-3}) \pi q^2 t_e \sum_{i=1}^{3} k_i P_i^{CR} R_i \end{aligned}\right\} \quad (9)$$

where q is the radius of the plastic container in cm (Fig. 6), k_i is the branching ratio in %, A_c^{222} $(Bq.cm^{-3})$ is the radon activity per unit volume.

The corresponding density of tracks (tracks $cm^{-2}.s^{-1}$) registered on the CR-39 SSNTD due to the α-particles of the radon group is:

$$\rho_T^{CR}\left(^{222}R_n\right) = A_c^{222}(Bq.cm^{-3}) \sum_{i=1}^{3} k_i P_i^{CR} R_i. \quad (10)$$

Similarly, the density of tracks (tracks $cm^{-2}.s^{-1}$) due to the α-particles of thoron family, registered on the CR-39 SSNTD is:

$$\rho_T^{CR}\left(^{220}R_n\right) = A_c^{220}\,(Bq.cm^{-3}) \sum_{i=1}^{4} k_i P_i^{CR} R_i \quad (11)$$

where $A_c^{220}(Bq.cm^{-3})$ is the thoron activity per unit volume.

The global density of tracks due to the α-particles of the radon and thoron series, registered on the CR-39 SSNTD is then:

$$\rho_G^{CR} = A_c^{222}(Bq.cm^{-3}) \left[\sum_{i=1}^{3} k_i\, P_i^{CR} R_i + Ac220Ac222i{=}14ki\, PiCR\, Ri \right] \quad (12)$$

Let P^{LR} represent the probability for an emitted α-particle to reach and be registered on the LR-115 SSNTD.

$$P^{LR} = \int_{R_{min}}^{R_{max}} [1 - cos\theta_c^1\,(x)]\, dx \quad (13)$$

where θ_c^1 is the critical angle of etching, which depends on the residual LR-115 SSNTD thickness.

R_{min} and R_{max} are the α-particle ranges in the sample which correspond to the lower and upper ends of the energy window and depend on the residual thickness of the LR-115 SSNTD [14].

Consequently, the density of tracks (tracks $cm^{-2}.S^{-1}$), due to the α-particles of the radon group, registered on the LR-115 SSNTD is given by:

$$\rho_T^{LR}(^{222}R_n) = A_c^{220}(Bq.cm^{-3}) 3P^{LR} \Delta R \quad (14)$$

where $\Delta R = R_{max} - R_{min}$.

Similarly, the density of tracks (track $cm^{-2}.S^{-1}$) due to the α-particles of the thoron group, registered on the LR-115 SSNTD is:

$$\rho_T^{LR}\left(^{220}R_n\right) = A_c^{220}(Bq.cm^{-3}) 4P^{LR} \Delta R\,. \quad (15)$$

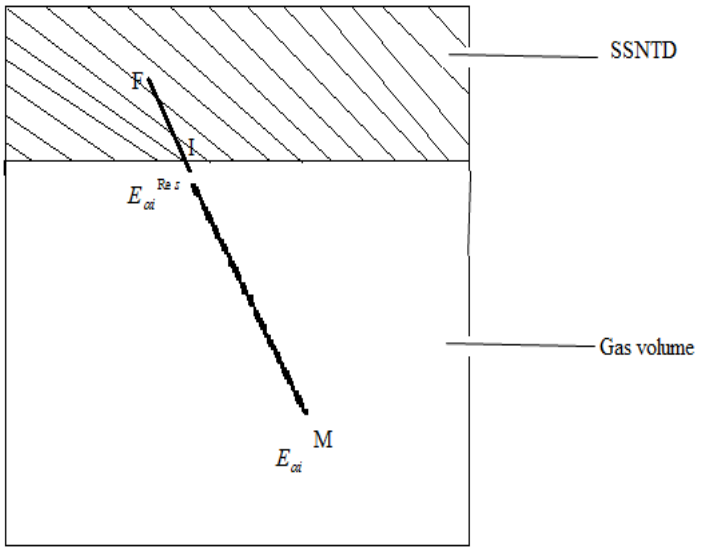

FIG. 6. Diagram illustrating primary trajectory of an α-particle inside the gas volume (MI = X) and SSNTD (IF = RD). $E_{\alpha i}$ is the initial energy of the α-particle and $E_{\alpha i}^{Res}$ is its residual energy on reaching point I.

The global density of tracks (tracks $cm^{-2}.S^{-1}$) due to the α-particles of the radon and thoron series, registered on the LR-115 SSNTD is equal to:

$$\rho_G^{LR} = A_c^{222}(Bq.cm^{-3})(3P^{LR}\Delta R + 4P^{LR}\Delta R\ \frac{A_c^{220}}{A_c^{222}}) \quad (16)$$

Combining equations (12) and (16), we obtained the following relationship between track densities and thoron to radon ratio.

$$\frac{\rho_G^{CR}}{\rho_G^{LR}} = \frac{\sum_{i=1}^{3} k_i P_i^{cR} R_i + \frac{A_c^{220}}{A_c^{222}} \sum_{i=1}^{4} k_i P_i^{cR} R_i}{3P^{LR}\Delta R + 4P^{LR}\,\Delta R\,\frac{A_c^{220}}{A_c^{222}}}. \quad (17)$$

By measuring ρ_G^{CR} *and* ρ_G^{LR} and knowing the values of P_i^{CR} and P^{LR} from Tables 1 and 2, respectively, one can determine the $\frac{A_c^{220}}{A_c^{222}}$ ratio using Eq. 17 and consequently the thoron A_c^{220} and radon A_c^{222} activities of the studied water samples by substituting Eq. 18 into Eq. 16.

From Eq. 17, one can determine the $\frac{A_c^{220}}{A_c^{222}}$ ratio as follows,

$$\frac{A_C^{220}}{A_C^{222}} = \frac{\sum_{i=1}^{3} K_i P_i^{CR} R_i - 3P^{LR}\Delta R\,\frac{\rho_G^{CR}}{\rho_G^{LR}}}{4P^{LR}\Delta R\,\frac{\rho_G^{CR}}{\rho_G^{LR}} - \sum_{i=1}^{4} K_i P_i^{CR} R_i}. \quad (18)$$

TABLE 1. Data obtained for the probability (P_i^{CR}) for radon group α -particles and thoron group α -particles to be registered on the CR-39 SSNTD for the gas volume of the α -particles of energy $E_{\alpha i}$ and *index* i in the gas volume [12].

Nuclides	$E_{\alpha i}$ (MeV)	R_i (cm)	$P_i^{CR} \times 10^{-3}$	k_j
Radon group α -particles				
^{222}Rn	5.49	3.90	2.871	1
^{218}Po	6.00	4.65	3.383	1
^{214}Po	7.68	6.65	4.440	1
Thoron group α- particles				
^{220}Rn	6.28	4.80	3.391	1
^{216}Po	6.78	5.45	3.433	1
^{212}Bi	6.08	4.75	3.527	0.36
^{212}Po	8.78	8.36	5.711	0.64

TABLE 2. Values of the probability (PLR) for the α -particles of the radon and thoron groups to be registered on the LR-115 SSNTD for different residual thicknesses for (LR-115 films) for the gas volume of the water samples. R_{min} and R_{max} are the α -particle ranges in the gas volume which correspond to the lower and upper ends of the energy window [12].

Residual thickness (μm)	R_{min} (cm)	R_{max} (cm)	$P^{LR} \times 10^{-3}$
3	0.46	3.83	203.299
4	0.61	3.52	11.302
5	0.80	3.44	4.329
6	0.98	2.71	1.536
7	1.07	2.66	1.405
8	1.29	2.53	1.336
9	1.42	2.31	0.267
10	1.60	2.02	0.191

The activity concentrations in groundwater samples ranged from 3050.49 to 90798.69 Bq/m^3 and from 660.76 to 57181.68 Bq/m^3 for ^{222}Rn and ^{220}Rn, respectively. The frequency distribution analyses are shown on Figs. 7 and 8 for track densities on the CR-39 and LR-115 detectors, respectively. The error on track density counting is smaller than 7% for the samples studied.

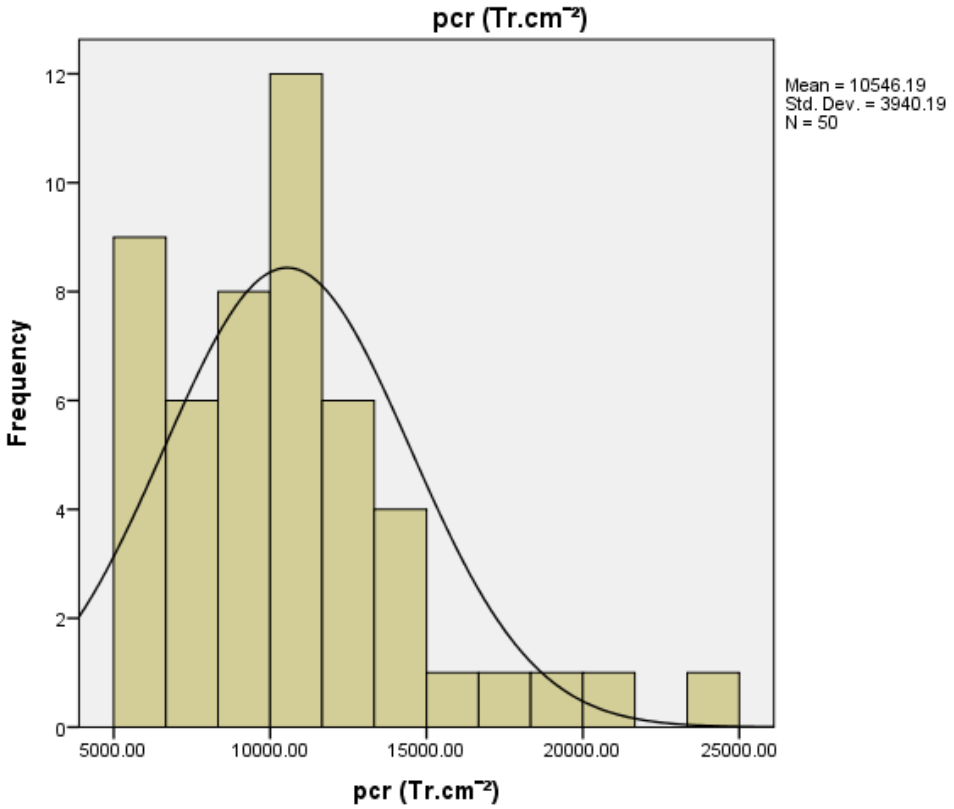

FIG. 7. Frequency curve for track density of radon in CR-39.

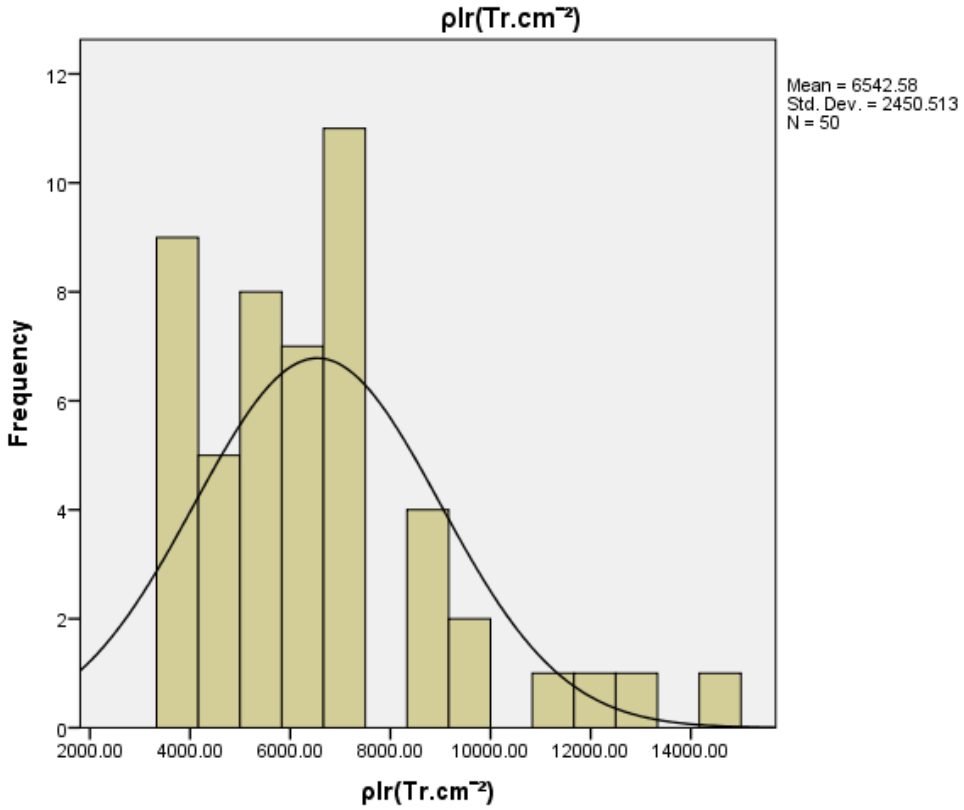

FIG. 8. Frequency curve for track density of radon in LR-115.

Calculation of Annual Effective Dose

The annual effective doses due to the intake of radon were calculated from the mean activity concentration using the following equation [15]:

$$E_{Rn} = DF_{Rn}.I_w.A_{Rn} \quad (19)$$

where DF_{Rn} is the effective dose per unit intake of radon in water, taken as 10^{-8} Sv/Bq for adults and $2X10^{-8}$ Sv/Bq for children from UNSCEAR 1993 report [16] and I_w is the water consumption rate, taken to be 2 litres per day from WHO report [17].

Results and Discussion

The values of the annual effective dose per person caused by different drinking groundwater samples in this study are presented in Table 3. The estimated total annual effective dose for children ranged from 71 μSv/y from drinking water of sample code GW 031 to 1326 μSv/y from drinking water of sample code GW006, with an average of (273) μSv/y, while for adults the total annual effective dose ranged from 35 μSv/y from drinking water of sample code GW031 to 663 μSv/y from drinking water of sample code GW006, with an average (136) μSv/y.

It is also noted from the results that among the 50 samples analyzed, the water sample from Panseke area recorded the highest ^{222}Rn concentration and the corresponding annual effective dose among all the other water samples.

More than 90% of the water samples resulted in annual effective doses for children above the 0.1mSv/y safe limit and 80% of the annual effective doses for adults were found to be above the safe limit of 0.1 mSv/y recommended by World Health Organization [18] and EU Council [8].

The results obtained showed that radon in drinking water could constitute a radiological concern for people using the areas and further research should be conducted to determine the prevalence and whether remediation action would be required.

TABLE 3. Results of annual effective dose in groundwater samples

SAMPLE CODE	LATITUDE	LONGITUDE	$^{222}A(Bq.m^{-3})$	±Error	$^{222}A(Bq.L^{-1})$	Annual effective dose ingestion (µSv/year) for children	Annual effective dose ingestion (µSv/year) for adults
GW 001	7.1743	3.35787	15692.01	±864.00	15.69	229.1	114.55
GW002	7.13982	3.34797	20044.33	±1718.00	20.04	292.65	146.32
GW003	7.16213	3.35272	38315.87	±977.00	38.32	559.41	279.71
GW004	7.23027	3.43965	40342.13	±1829.00	40.34	589	294.5
GW005	7.18316	3.3476	49679.72	±1766.00	49.68	725.32	362.66
GW006	7.12097	3.32184	90798.69	±3838.00	90.80	1325.66	662.83
GW007	7.18172	3.36091	46721.01	±823.00	46.72	682.13	341.06
GW008	7.16676	3.34329	51458.57	±1786.00	51.46	751.3	375.65
GW009	7.17234	3.34977	78330.88	±2003.00	78.33	1143.63	571.82
GW010	7.16853	3.3592	41390.51	±2437.00	41.39	604.3	302.15
GW011	7.15634	3.35335	15789.83	±465.00	15.79	230.53	115.27
GW012	7.15638	3.34943	27532.87	±444.00	27.53	401.98	200.99
GW013	7.19343	3.35785	41049.10	±2240.00	41.05	599.32	299.66
GW014	7.13489	3.34268	58084.87	±4081.00	58.08	848.04	424.02
GW015	7.1473	3.3658	46225.88	±1181.00	46.23	674.9	337.45
GW016	7.16248	3.37185	39018.71	±1250.00	39.02	569.67	284.84
GW017	7.15296	3.36709	12140.36	±556.00	12.14	177.25	88.62
GW018	7.1721	3.37229	27954.36	±1125.00	27.95	408.13	204.07
GW019	7.177	3.39131	46525.38	±1238.00	46.53	679.27	339.64
GW020	7.18759	3.437	44844.35	±827.00	44.84	654.73	327.36
GW021	7.14334	3.37364	23400.36	±953.00	23.40	341.65	170.82
GW022	7.13674	3.30494	50278.71	±2509.00	50.28	734.07	367.03
GW023	7.13946	3.33029	22024.86	±1618.00	22.02	321.56	160.78
GW024	7.15733	3.32958	23498.17	±418.00	23.50	343.07	171.54
GW025	7.14647	3.3161	16095.37	±693.00	16.10	234.99	117.5
GW026	7.11752	3.33147	54331.54	±1353.00	54.33	793.24	396.62

SAMPLE CODE	LATITUDE	LONGITUDE	$^{222}A(Bq.m^{-3})$	±Error	$^{222}A(Bq.L^{-1})$	Annual effective dose ingestion (µSv/year) for children	Annual effective dose ingestion (µSv/year) for adults
GW027	7.19266	3.45426	50376.53	±1076.00	50.38	735.5	367.75
GW028	7.15388	3.34628	52552.69	±3229.00	52.55	767.27	383.63
GW029	7.15204	3.34529	13418.03	±784.00	13.42	195.9	97.95
GW030	7.17844	3.40159	20479.45	±416.00	20.48	299	149.5
GW031	7.2044	3.34587	4829.33	±279.00	4.83	70.51	35.25
GW032	7.2022	3.36179	48597.68	±2077.00	48.60	709.53	354.76
GW033	7.15711	3.34572	33486.53	±2331.00	33.49	488.9	244.45
GW034	7.16079	3.35528	22024.86	±2163.00	22.02	321.56	160.78
GW035	7.15854	3.3527	36237.52	±1352.00	36.24	529.07	264.53
GW036	7.15233	3.33974	23803.71	±1675.00	23.80	347.53	173.77
GW037	7.14853	3.35883	8582.66	±822.00	8.58	125.31	62.65
GW038	7.14492	3.34972	25778.19	±1712.00	25.78	376.36	188.18
GW039	7.16625	3.353303	32985.36	±1154.00	32.99	481.59	240.79
GW040	7.16927	3.35122	27954.36	±2203.00	27.95	408.13	204.07
GW041	7.13633	3.35022	35161.53	±2809.00	35.16	513.36	256.68
GW042	7.145	3.3511	20044.33	±1412.00	20.04	292.65	146.32
GW043	7.14471	3.35035	12335.99	±414.00	12.34	180.11	90.05
GW044	7.17578	3.36225	56306.02	±1463.00	56.31	822.07	411.03
GW045	7.15855	3.34456	20723.02	±691.00	20.72	302.56	151.28
GW046	7.15809	3.34825	18257.52	±1636.00	18.26	266.56	133.28
GW047	7.12508	3.34173	27654.86	±1784.00	27.65	403.76	201.88
GW048	7.16201	3.36243	21523.69	±1023.00	21.52	314.25	157.12
d.wtater			3050.49	±111.00	3.05	44.54	22.27
GW050	7.14017	3.33817	22024.86	±1035.00	22.02	321.56	160.78

Conclusion

Two types of Solid State Nuclear Track Detector (SSNTD); i.e., CR-39 and LR-115 type II, were used in this study to evaluate the concentrations of ^{222}Rn and ^{220}Rn in groundwater samples from different locations in Abeokuta. This technique has the advantages of being simple, accurate, inexpensive and non-destructive and does not need the use of any standard for its calibration. The results showed a range of ^{222}Rn concentrations between 3050.49 and 90798.69 Bq/m^3. Generally, there was a higher concentration of ^{222}Rn in the well-water samples compared to ^{220}Rn, although there were exceptional cases where ^{220}Rn concentrations were higher than those of ^{222}Rn. A well in Panseke area recorded the highest ^{222}Rn concentration (90798.69 Bq/m^3).Other areas with high radon concentration values are Sapon (52552.69 Bq/m^3), Okearegba (56306.02 Bq/m^3) and Ake (38315.87 Bq/m^3). The results of ^{222}Rn concentrations agree well with those obtained earlier by [19] using RAD7 connected to a bubbling kit to degas radon from water samples.

Going by the results of this study and the strong dependence of the populace on groundwater, it is concluded that water consumption may be a relevant radiological exposure pathway among some of the inhabitants of Abeokuta. It is therefore pertinent to recommend that more consideration should be given to further study of radon in indoor air and drinking water in different parts of Abeokuta with a view to ascertain prevalence and remediation required. The results of this study revealed that many of the groundwater samples in the study area have high levels of ^{222}Rn. Considering that a large population of Nigerians derive water for drinking and other domestic uses from underground sources, it is recommended that study of radon concentration in water and indoor air should be promoted among researchers, e.g. by giving grants for large-scale regional or national surveys. The SSNTD method for radon studies and for measurement of other natural radionuclides should be further encouraged.

References

[1] Veeger, A.I. and Ruderman, N.C., Ground Water, 36(4) (1998) 596.

[2] Juntunen, R., "Uranium and Radon in Wells Drilled into Bedrock in Southern Finland", Report of Investigation, Helsinki: Geological Survey of Finland, 98 (1991).

[3] Salih, I., Bäckström, M., Karlsson, S., Lund, E. and Pettersson, H.B.L., Applied Radiation and Isotopes, 60(1) (2004) 99.

[4] Salonen, L., Future Groundwater Resources at Risk: IAHS Publ., 222 (1994) 71.

[5] Akerblom, G. and Lindgren, J., European Geologist, 5 (1997) 13.

[6] WHO, "Guidelines for Drinking Water Quality". Recommendations, Vol. 1, 3rd Edition. (World Health Organization, Geneva, 2004).

[7] National Research Council, "Risk Assessment of Radon in Drinking Water", (Washington D.C.: National Academy Press, 1999).

[8] European Commission, Official Journal of the European Commission, Official J L 330 (1998).

[9] Kendall, G.M., Fell, T.P. and Phipps, A.W., Radiological Protection Bulletin, 97 (1988) 7.

[10] Swedjemark, G.A. and Linden, A.H., Radiation Protection Dosimetry, 80(4) (1998) 405.

[11] Fleischer, R.L., Price, P.B. and Walker, R.K., "Nuclear Tracks in Solids, Principles and Applications", Berkeley, (California: University of California, 1975).

[12] Misdaq, M.A. and Satif, C., J. Radioanal. Nucl. Chem., 207 (1996) 107.

[13] Misdaq, M.A., Gilane, M., Ouguidu, J. and Outeqabit, K., Radiat. Prot. Dosim., 142 (2000) 136.

[14] Somogyi, G., 15th Int. Symp. on Autoradiography, Matarfured, Hungary, 20-23 Oct., (1986).

[15] IAEA, "Water for People, Water for Life", UN World Water Development Report, 2001.

[16] United Nations Scientific Committee on the Effects of Atomic Radiation, UNSCEAR. "Sources and Effects of Ionizing Radiation", UNSCEAR Report to the General Assembly with Scientific Annexes, United Nations, New York, (1993).

[17] World Health Organization, WHO, "Guidelines for Drinking Water Quality", Vol.1, 2nd ed. (WHO, Geneva, 1993).

[18] WHO, "Guidelines for Drinking Water Quality", 3rd Ed., (WHO, Geneva, 2008).

[19] Oni, O.M., Oladapo, O.O., Amuda, D.B, Oni, E.A., Adelodun, A.O., Adewale, K.Y. and Fasina, M.O., Nigerian Journal of Physics, 25(1) (2014).